Gas-Phase Reactions of Chlorine Atoms and ClO Radicals with Dimethyl Sulfide. Rate Coefficients and Temperature Dependences

Y. Díaz-de-Mera, A. Aranda, D. Rodríguez, R. López, B. Cabañas, and E. Martínez*

Facultad de Químicas, Campus Universitario, s/n. 13071 Ciudad Real, Spain

Received: December 18, 2001; In Final Form: April 5, 2002

The results of a discharge flow-mass spectrometric (DF-MS) kinetic study of the reaction between Cl and dimethylsulfide (DMS) (1) over the temperature range 259−364 K at low total pressure between 0.5 and 1 Torr with helium as carrier gas are reported. At room temperature and 1.0 Torr the main products of reaction 1 correspond to an abstraction channel leading to HCl and CH_3SCH_2 with $k(1) = (6.9 \pm 1.3) \times 10^{-11}$ cm^3 molecule^{-1} s^{-1}. The association channel has also been confirmed by mass spectroscopic detection of the adduct $CH_3S(Cl)CH_3$ with a yield <0.05 under the experimental conditions used. It is now shown that the abstraction channel requires a slight activation energy, $k(1) = (2.0 \pm 1.2) \times 10^{-10} \exp[-(332 \pm 173)/T]$ cm^3 molecule^{-1} s^{-1}. The kinetics and mechanism of the reaction ClO + DMS → products (2) over the temperature range 259−335 K at total pressures between 0.5 and 2 Torr have also been studied by DF-MS. By mass spectroscopic calibration of dimethyl sulfoxide, DMSO, the branching ratio of the channel leading to this product has been measured (0.90 ± 0.49). The rate constant of reaction 2 has been measured under pseudo-first-order conditions in excess of DMS over ClO: $k(2) = (1.2 \pm 0.7) \times 10^{-15} \exp[(354 \pm 163)/T]$ cm^3 molecule^{-1} s^{-1} with $k(2) = (3.9 \pm 1.2) \times 10^{-15}$ cm^3 molecule^{-1} s^{-1} at 298 K. The reaction is postulated to proceed through a channel involving a long-lived intermediate $[CH_3S(OCl)CH_3]$* which may decompose back to reactants or to products. Finally, the atmospheric implications through the DMS chemistry of both reactions are discussed.

Introduction

Dimethyl sulfide (CH_3SCH_3) is recognized as the natural sulfur compound of greatest interest to atmospheric chemistry.[1,2] The largest source of sulfur in the atmosphere (>60% of the total emission) is the SO_2 released by fossil fuel combustion and industrial processes. The second largest source is the oceanic emission of DMS by marine phytoplankton, exceeding the anthropogenic sulfur emissions in the southern hemisphere.[3,4] Tropospheric oxidation of DMS produces dimethyl sulfoxide (CH_3SOCH_3), dimethyl sulfone ($CH_3SO_2CH_3$), sulfinic acid ($CH_3S(O)OH$), methanesulfonic acid (CH_3SO_2 OH), SO_2, and sulfuric acid with yields dependent on temperature and NO_x levels[5−7] and it seems to be the major source of cloud condensation nuclei in the marine troposphere.[8] The sulfur aerosols could significantly influence the radiative solar balance on the Earth's surface representing, thus, a biological climate regulation.[8,9] So, DMS impacts, both in the gas phase and through aerosols, are currently subject of study in box models, laboratory, and field campaigns.[10,11]

The main known sinks for DMS in the troposphere are the reaction with OH radicals[12,13] and, to a minor extent, the reaction with NO_3 under night-time conditions.[14] Recent studies indicate that halogen atoms and halogen oxides may also be important as sinks for DMS.[15,16] Indeed, in marine areas, where $ClNO_2$ generated by heterogeneous reaction of N_2O_5 vapor with moist NaCl may raise Cl atoms concentrations up to 10^4 atom cm^{-3}, the DMS degradation initiated by Cl atoms may be competitive compared to OH and NO_3 reactions.[17] In this sense, several experimental[16,18−22] and ab initio studies[23,24] have been reported on the reaction of Cl with DMS, for which the following channels are possible:

$$Cl + CH_3SCH_3 \rightarrow HCl + CH_3SCH_2 \quad (1a)$$

$$Cl + CH_3SCH_3 \rightarrow [(CH_3)_2SCl]^* \quad (1b)$$

$$[(CH_3)_2SCl]^* + M \rightarrow CH_3SCl + CH_3 + M \quad (1b1)$$

$$[(CH_3)_2SCl]^* + M \rightarrow CH_3Cl + CH_3S + M \quad (1b2)$$

$$[(CH_3)_2SCl]^* + M \rightarrow [(CH_3)_2SCl] + M \quad (1b3)$$

The Cl + DMS reaction proceeds via two distinct channels, a pressure-independent channel forming HCl + CH_3SCH_2, (1a), and an adduct-forming pressure-dependent channel, (1b).[14,19] As demonstrated by Zhao et al.[21] using the TDLAS technique, the yield of CH_3 through reaction 1b1 is less than 0.02 (upper limit), which is also expected from the theoretical results of Resende et al.[23] From the observations of Langer et al.[25] and the potential energy surfaces[23] a net production of CH_3Cl and CH_3S (1b2) is also improbable under kinetic conditions. Finally, the rate coefficient of channel (1b3) increases with pressure, approaching its high-pressure limit between 150 and 700 Torr and being competitive to the abstraction channel.

Nevertheless, all the previous laboratory studies were mainly focused on the high-pressure regime (3 Torr-atmospheric pressure) except for the work of Butkovskaya et al.[20] at 1.0 Torr who studied the products and mechanism but not the kinetics. Up to now, the branching ratio for the abstraction

* Corresponding author. E-mail: emartine@qifi-cr.uclm.es. Fax: 34 26295318.

10.1021/jp014570c CCC: $22.00
Published on Web 08/16/2002

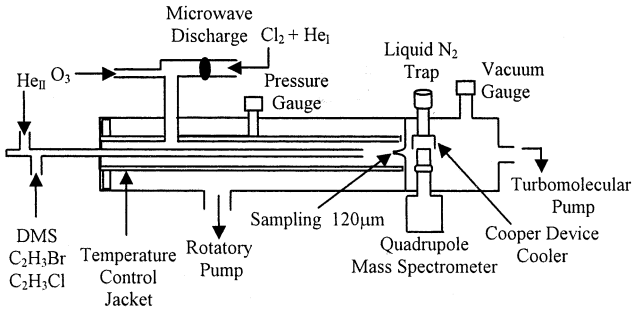

Figure 1. Schematic view of the experimental setup.

channel, (1a), is not clear, and direct information concerning the abstraction process is not available. The technique used in this work seems more appropriate to characterize reaction 1 in the low-pressure limit. Furthermore, the temperature dependence of the abstraction process has not been studied previously and so it is reported here for the first time.

In relation to the halogen oxides XO (X = I, Br, and Cl), they can also be formed in the troposphere from the photo oxidation of halogenated hydrocarbons. Although their concentrations in the troposphere are not well-known, modeling studies suggest values up to 10^6 molecule cm^{-3}, [26] showing that their reactions toward DMS ought to be measured in order to evaluate the potential contribution to the removal of DMS. Studies of IO + DMS kinetics demonstrate that the oxidation of DMS by IO is negligible ($k_{298} = (1.6 \pm 0.3) \times 10^{-14}$ cm^3 $molecule^{-1}$ s^{-1})[27] compared to the oxidation by OH in marine atmosphere. On the other hand, the BrO + DMS reaction is relatively fast ($k_{298} = (4.4 \pm 0.7) \times 10^{-13}$ cm^3 $molecule^{-1}$ s^{-1}), constituting a potential sink for DMS and a source of DMSO in the marine boundary layer.[28−30] Only a room temperature study at 1 Torr of the ClO−DMS reaction is available[31] with $k = (9.5 \pm 2.0) \times 10^{-15}$ cm^3 $molecule^{-1}$ s^{-1} and a qualitative discussion of products. In this work we report now a wider kinetic and mechanistic study with the quantitative determination of the products of reaction. The influence of temperature on the kinetic rate constant is reported for the first time.

Experimental Section

The kinetic experiments were carried out using the discharge flow-mass spectrometry technique (DF-MS). The apparatus is shown schematically in Figure 1. The flow reactor was a 100 cm long Pyrex tube with 2.7 cm internal diameter provided with a jacket for the thermostating liquid circulation (SilOil). The movable injector was 120 cm long and 1 cm i.d. Both of them were coated with halocarbon wax in order to reduce the heterogeneous wall reactions. The reactor was pumped by means of a rotary pump and the pressure was measured with a 10 Torr full-scale capacitance gauge. The flows of the helium carrier gas in the reactor and the injector were regulated and measured with mass flow controllers to control concentrations and pumping speeds. All the reactants were diluted in helium and stored in balloons of known volume. Concentrations of reactants in the reactor were calculated from the pressure decrease rate inside the storage flasks. Both radical and molecular species were sampled from the reactor through a glass cone with an orifice of 120 μm diameter and analyzed by a quadrupole mass spectrometer (VG Smart IQ^+) with electron impact ion source. The energy of ionizing electrons was typically 40 eV. The high vacuum chamber was pumped by means of a turbo-molecular pump (Varian 550V). For more details, see ref 32.

Cl atoms were produced by microwave discharge (2450 MHz) in Cl_2 diluted by He and then flowed into the main reactor through a Pyrex sidearm tube coated with phosphoric acid in order to increase the Cl_2 dissociation yield, which could be checked by mass spectrometry at $m/e = 70$, 72. The absolute concentration of Cl atoms was measured by a titration reaction with $BrCH{=}CH_2$ in excess,

$$Cl + BrCH{=}CH_2 \rightarrow ClCH{=}CH_2 + Br \qquad (3)$$

$$k(3) = 1.4 \times 10^{-10}\ cm^3\ molecule^{-1}\ s^{-1}\ (ref\ 33)$$

and mass spectrometric detection of $BrCH{=}CH_2$ or $ClCH{=}CH_2$ at their parent peaks, $m/e = 107$ and $m/e = 62$, respectively.

ClO radicals were generated by the reaction with ozone,

$$Cl + O_3 \rightarrow ClO + O_2 \qquad (4)$$

$$k(4) = 1.2 \times 10^{-11}\ cm^3\ molecule^{-1}\ s^{-1}\ (ref\ 34)$$

ClO radicals were produced in an excess of O_3 ($m/e = 48$) to ensure complete consumption of the Cl atoms, to avoid the interference of Cl + DMS reaction. O_3 was generated by an ozonizer (Ozogas, 5 g/h), collected in a liquid N_2 trap and degassed before stored diluted in helium. This ozone was used only within an experimental session to avoid the decomposition of O_3 into O_2.

The knowledge of absolute concentration of ClO is not necessary for calculations under pseudo-first-order conditions but a calibration of the M.S. signal was accomplished by chemical conversion to NO_2 with NO in excess

$$ClO + NO \rightarrow NO_2 + Cl \qquad (5)$$

$$k(5) = 1.7 \times 10^{-11}\ cm^3\ molecule^{-1}\ s^{-1}\ (ref\ 34)$$

and mass spectrometric detection of NO_2 at its parent peak, $m/e = 46$. Titration reaction was performed in an excess of Cl atoms over O_3 to ensure the complete consumption of ozone and thus avoid the regeneration of ClO via reaction 4 or a contribution to NO_2 by

$$NO + O_3 \rightarrow NO_2 + O_2 \qquad (6)$$

$$k(6) = 1.8 \times 10^{-14}\ cm^3\ molecule^{-1}\ s^{-1}\ (ref\ 34)$$

Generally, this titration sequence was in agreement with the direct measurement assuming that all Cl atoms produced ClO radicals.

DMS was purified by trap-to-trap distillation, and added to the reactor through the sliding injector. For ClO + DMS reaction, DMS was stored without dilution in helium in order to achieve concentrations as high as 5×10^{15} molecule cm^{-3} in the reactor. The detection limits for DMS, Cl_2, and ClO were 4×10^9 molecule cm^{-3}, 1×10^{10} molecule cm^{-3}, and 2×10^{10} molecule cm^{-3}, respectively.

The purities of the chemicals were as follows: Cl_2 (Praxair, >99.8%), O_2 (Praxair, 99.999%), CH_3SCH_3 (Aldrich, >99%), C_2H_3Br (Aldrich, 98%), C_2H_3Cl (Fluka, ≥99.5%), NO (Praxair, ≥99%), NO_2 (Praxair, ≥99.5%), and He (Praxair, 99.999%).

Results

Reaction Cl + DMS. The kinetic experiments were carried out under pseudo-first-order conditions with Cl atoms in excess over DMS molecules with a ratio [Cl]/[DMS] from 10 to 100. The experimental conditions are summarized in Table 1. The results in this work include $\pm 2\sigma$ and 10% of the absolute

TABLE 1: Experimental Conditions for the Determination of the Rate Coefficients

	Cl + DMS	ClO + DMS
T/K	259−364	259−335
p/Torr	0.5, 1.0	0.5, 1.0, 2.0
flow velocity/m s^{-1}	25−30	5−7
reaction time/ms	0−15	0−100
$[Cl_2]$/molecule cm^{-3}	$(0.5-7.0) \times 10^{13}$	$(0.7-3.0) \times 10^{12}$
[Cl]/atom cm^{-3}	$(0.1-1.0) \times 10^{13}$	$(0.8-1.0) \times 10^{12}$
$[O_3]$/molecule cm^{-3}		$(2.0-5.0) \times 10^{13}$
[ClO]/molecule cm^{-3}		approx. 1.0×10^{12}
[DMS]/molecule cm^{-3}	$(0.5-1.0) \times 10^{11}$	$(0.4-5.0) \times 10^{15}$

magnitude to cover systematic errors, giving a final confidence limit around 95%.

No reaction was observed between DMS and Cl_2 (precursor of Cl atoms) within the short contact time used in the experiments (less than 15 ms). To check the heterogeneous wall losses of reactants, additional experiments were carried out separately before each kinetic run. Wall losses in both the injector and the reactor ($k_{wi} + k_{wr} = 6 \pm 4\ s^{-1}$) were measured conjunctly by titration of Cl atoms (from the fixed port in the beginning of the reactor) with $BrCH{=}CH_2$ (coming from the injector) at different positions. k_{wr}, the loss rate constant in the reactor wall, was measured in separate experiments, with Cl atoms entering the reactor through the sliding injector and the titrating C_2H_3Br through a fixed lateral port near the end of the reactor, $k_{wr} = 3 \pm 2\ s^{-1}$, which also allows us to calculate $k_{wi} = 3 \pm 6\ s^{-1}$. During a kinetic run, for increasing times of reaction, the exposure of Cl atoms to the inner surface of the reactor is always the same and the experimental rate constant may be considered as not k_{wr} dependent. On the other hand, the injector wall decreases with increasing times of reaction and so it should be included in the kinetic analysis as a source of Cl atoms. However, this process is very slow and for the short time scale of our experiments, Cl concentration may be considered constant, which enables the pseudo-first-order treatment. The average [Cl] was used to minimize this small variation due to wall effects during any experiment.

For DMS, entering the reactor from the sliding injector, k_w in the reactor wall was achieved by monitoring its parent peak ($m/e = 62$) at different position of the injector. The measured values were $k_w = 5 \pm 4\ s^{-1}$ for the range of temperatures and pressures studied.

The temporal decay of the DMS concentration was monitored by mass spectrometry at $m/e = 62$ (CH_3SCH_3) and fitted to the kinetic equation:

$$\ln([DMS]_0/[DMS]_t) = (k'(1) + k_w)t \quad \text{with } k'(1) = k(1)\,[Cl] \qquad \text{(I)}$$

For each temperature, several temporal profiles with different initial Cl concentrations were followed. Typical logarithmic decays of the intensity of DMS signal as a function of reaction time are shown in Figure 2. As typified by these data, all the results are consistent with eq I and the pseudo-first-order kinetic rate constants $k'(1)$ may be calculated from the slope. The obtained experimental values for $k'(1)$ are corrected for axial diffusion of DMS using the diffusion coefficient:[35]

$$k' = k'_{exp}(1 + k'_{exp} \times D_{DMS/He}/v^2) \qquad \text{(II)}$$

where v is the linear velocity of the gas mixture in the reactor (cm s^{-1}) and $D_{DMS/He}$ is the diffusion coefficient of DMS in He ($cm^2\ s^{-1}$) calculated from the volumes of atomic diffusion.[36] $D_{DMS/He}$ has been obtained for each experimental condition because of its dependence on temperature and pressure, with values ranging from 225 to 400 $cm^2\ s^{-1}$ and $D_{DMS/He} = 290$ $cm^2\ s^{-1}$ at room temperature and 1.0 Torr. The correction on k' due to the axial diffusion was around 2% and 5% for experiments at 1.0 and 0.5 Torr, respectively.

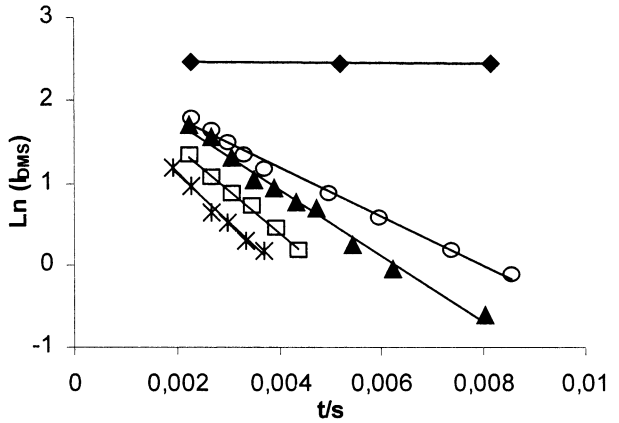

Figure 2. Typical pseudo-first order decays of DMS for the Cl + DMS reaction at 298 K and 1 Torr: [Cl] = 0 (◆); 1.78 (○); 2.88 (▲); 4.56 (□); and 6.77 (*)10^{12} molecule cm^{-3}.

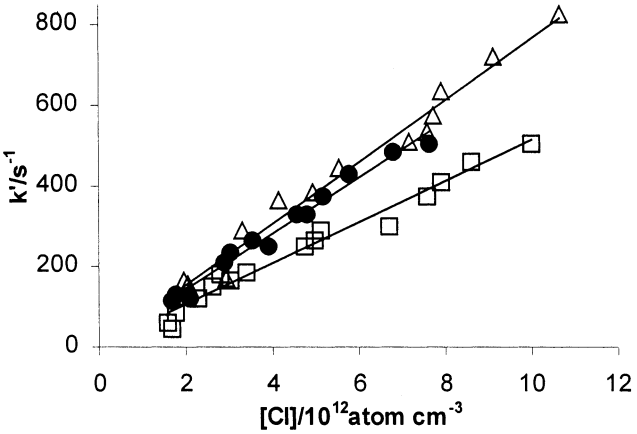

Figure 3. Second-order plot for the Cl + DMS reaction at 1 Torr: T = 259 (□); 298 (●); and 364 (△) K.

TABLE 2: Summary of Second-Order Rate Constants for Cl + DMS and ClO + DMS Reactions at Different Temperatures and Pressures [$k(1)$ in units of 10^{-11} cm^3 $molecule^{-1}\ s^{-1}$, and k(2) in units of 10^{-15} cm^3 $molecule^{-1}\ s^{-1}$]

Cl + DMS				
$T = 259$ K	$T = 283$ K	$T = 298$ K		T = 364 K
$p = 1$ Torr	$p = 1$ Torr	$p = 0.5$ Torr	$p = 1$ Torr	$p = 1$ Torr
5.2 ± 1.2	6.4 ± 1.6	7.0 ± 2.1	6.9 ± 1.3	7.8 ± 1.4

ClO + DMS				
$T = 259$ K	$T = 298$ K			$T = 335$ K
$p = 1.0$ Torr	$p = 0.5$ Torr	$p = 1$ Torr	$p = 2$ Torr	$p = 1$ Torr
4.5 ± 2.4	4.0 ± 1.6	3.9 ± 1.2	4.5 ± 1.6	3.3 ± 1.7

The bimolecular rate coefficient of interest, $k(p,T)$, is evaluated from the slope of the $k'(1)$/[Cl] plot applying weighted least-squares fittings. Measured values for $k'(1)$ at different temperatures are plotted as a function of Cl concentration in Figure 3. In Table 2 we summarize the results for all the experimental conditions within the range of temperature 259−364 K. The reaction rate is found to increase slightly with increasing temperature. The Arrhenius equation applies to these results as it may be observed in Figure 4, where ln $k(1)$ is plotted versus1/T. A linear least-squares analysis of the data yields the activation

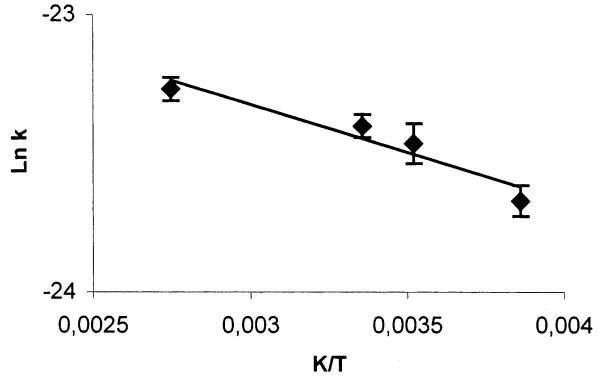

Figure 4. Temperature dependence of the rate constant for the reaction Cl + DMS.

energy, the preexponential factor and affords the calculation of the kinetic rate constant $k(1)$ through the following equation in the range 259−364 K:

$$k(1) = (2.0 \pm 1.2) \times 10^{-10} \exp[-(332 \pm 173)/T] \text{ cm}^3 \text{ molecule}^{-1} \text{ s}^{-1} \quad \text{(III)}$$

Concerning the pressure range studied (0.5−1 Torr), it was very short due to the limitations of the experimental conditions. We also tried higher pressures but the flow velocity was too slow to achieve enough time resolution for the kinetics. The obtained values at room temperature and the experimental error bars indicate that the reaction Cl + DMS is not quite sensitive to pressure changes within this limited range.

Reaction ClO + DMS. For this reaction the experiments were also carried out under pseudo-first-order kinetic conditions, but now the concentrations were inverted. The reaction was found to be very slow and the efficiency of the Cl_2 discharge in producing Cl atoms decreased with increasing Cl_2 concentrations, so ClO concentrations could not be enhanced high enough to obtain a temporal decay of DMS. Thus, DMS molecules in excess over ClO radicals with a ratio [DMS]/[ClO] from 400 to 5000 were used. The experimental conditions are summarized in Table 1.

As for the case of reaction Cl + DMS, the system was checked for losses of reactants separately. For DMS, which entered the reactor from the sliding injector, these losses were found negligible and its concentration remained essentially constant during the experiments. With regard to ClO radicals, k_w could be calculated by means of titration with NO (coming from the sliding injector) in the same way as described earlier for Cl. The values obtained under the different experimental conditions were almost constant and negligible, with an upper limit of $k_w < 2$ s^{-1}. Losses due to the gas-phase self-recombination of ClO were of no significance in the present study because of the low rate coefficient for this reaction at 1 Torr ($k = 1.6 \times 10^{-14}$ cm^3 molecule^{-1} s^{-1}).[37] The evolution of ClO concentration during a kinetic run was monitored at its M S. parent peak, $m/e = 51$, 53 and is governed by

$$\ln([\text{ClO}]_0/[\text{ClO}]_t) = (k'(2) + k_w)t \quad \text{with } k'(2) = k(2)\,[\text{DMS}] \quad \text{(IV)}$$

In Figure 5 some examples of ClO decays as a function of time are shown, where the pseudo-first-order kinetic rate constants were calculated from linear regression. Again the values of k' were corrected for axial diffusion as described for Cl + DMS reaction. The corrections on $k'(2)$ ranged from 1 to 5% depending on temperature and pressure conditions. The

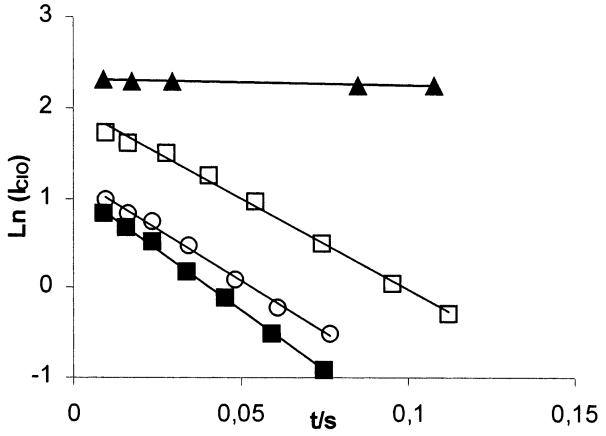

Figure 5. Examples of pseudo-first-order plots for the ClO + DMS reaction at 298 K and 1 Torr: [DMS] = 0 (▲); 0.92 (□); 2.35 (○); and 3.12 (■) 10^{15} molecule cm^{-3}.

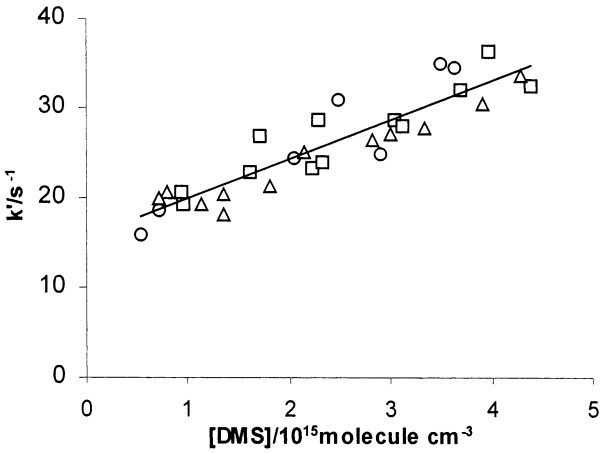

Figure 6. Second-order plot for the ClO + DMS reaction at 298 K. $p = 0.5$ (○), 1 (□), and 2 (△) Torr.

values for $k(2)$ were obtained from plots of $k(2)'$ versus [DMS], where a pure first-order behavior was observed. However the intercepts obtained at all the temperatures, 14 ± 4 s^{-1}, are higher than the rate of ClO wall losses in the absence of DMS. This effect is likely to occur due to a modification of the surface activity when DMS is present. Further information is found in the discussion section. A similar behavior was also reported in the flow tube study of BrO−DMS reaction.[28]

The results obtained at room temperature are shown in Figure 6 and the data obtained for all the experimental conditions are summarized in Table 2. As noted, the reaction rate decreases slightly as temperature increases as it may be seen in the corresponding Arrhenius form, Figure 7. From the obtained data we propose the next expression for $k(2)$ from 259 to 335 K:

$$k(2) = (1.2 \pm 0.7) \times 10^{-15} \exp[(354 \pm 163)/T] \text{ cm}^3 \text{ molecule}^{-1} \text{ s}^{-1} \quad \text{(V)}$$

Reaction 2 was studied within the pressure range 0.5−2.0 Torr. According to the results at room temperature, Figure 6, Table 2, no clear trend is found within this interval, though it could be masked within the error limits for such a small range of pressure.

Discussion

Reaction Cl + DMS. In this article we report the first study of the kinetics of reaction 1 at low pressure using an absolute

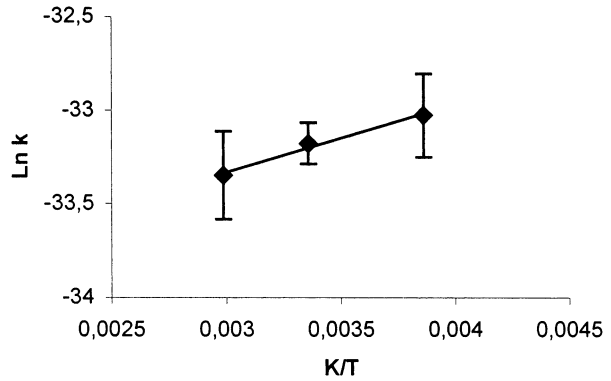

Figure 7. Temperature dependence of the rate constant for the reaction ClO + DMS.

technique. Under similar conditions, at $p \approx 3$ Torr, only a few experiments were reported with $k(1) = 1.8 \times 10^{-10}$ cm^3 molecule^{-1} s^{-1} within a study[19] mainly focused in the high-pressure limit with laser flash photolysis and resonance fluorescence for Cl.

It has been shown[19,20] that the reaction proceeds through two different pathways, an abstraction channel (1a), which is considered to be the main one at low pressure, and the formation of the corresponding adduct (1b), found to be stable enough as to show spectroscopic properties and follow different reactions under atmospheric conditions.[16]

Following the results of Stickel et al.[19] and Urbanski et al.,[16] even at high pressures the abstraction channel is significant as it could account for up to 50% of the reaction yield. However, the rate of the abstraction channels has not been properly isolated yet. Furthermore it is not clear whether the abstraction products proceed from a direct reaction involving only the Cl−H−S bonds or if they come from the re-location and cleavage in the excited adduct.

From this work the following observations should be taken into account. Concerning the products, the following peaks were observed by mass spectrometry, $m/e = 96, 98, 50, 52, 97, 99$. The signals at $m/e = 96, 98$ may correspond to CH_3SCH_2Cl (with different isotopic Cl), which would mean the propagation of the chain reaction in the presence of an excess of Cl_2

$$CH_3SCH_2 + Cl_2 \rightarrow CH_3SCH_2Cl + Cl \qquad (7)$$

$$k(7) = (7.1 \pm 2.0) \times 10^{-12}\,\text{cm}^3\,\text{molecule}^{-1}\,\text{s}^{-1}\ \text{(ref 20)}$$

The much less intense peaks at $m/e = 97, 99$ could be argued as the $M + 1$ signals in the mass spectrometer. Clearly this is not the case since the temporal evolution was clearly different. Signals at $m/e = 97, 99$ were formed from the very beginning of the reaction, while $m/e = 96$ and 98 seemed to require an induction time typical of the consecutive chain reaction. So the $m/e = 97, 99$ signals may be assigned to the adduct whose existence had been supported by ab initio studies[23] and directly observed through UV spectroscopy.[16] Peaks at $m/e = 50, 52$ are less intense and, as discussed previousl,y[20] they probably proceed from the breaking of CH_3SCH_2Cl in the M.S. ion source.

In some additional experiments lowering the Cl_2 concentrations from the radical source down to $\leq 5 \times 10^{11}$ molecule cm^{-3} the chain reaction is not propagated and radical−radical reactions could be confirmed by the detection of $(CH_3SCH_2)_2$ at $m/e = 122$. This observation shows that free CH_3SCH_2 must be present in the CH_3SCH_3 + Cl system. Furthermore, since HCl was observed even under high-pressure conditions[19] where the adduct must be deactivated, we may conclude that the abstraction products do not proceed from the decomposition of the excited adduct. From the relative intensity of the products signals, considering the same sensitivity under M.S. detection for CH_3SCH_2Cl and $CH_3S(Cl)CH_3$, the yield of the adduct at 1 Torr total pressure and room temperature has been estimated as less than 5%. This is consistent with the results of Butkovskaya et al.[20] who found a unity yield on the abstraction channel. That conclusion was obtained by verifying that the consumption of Cl_2 and DMS due to the chain propagation of the reaction (reactions 1a and 7) was approximately equal. A 0.98 HCl yield was also found by Stickel et al.[19] when using a 0.6 Torr of CO_2.

The temperature dependence of the rate constants obtained in this study shows a slight activation energy of 2.8 ± 1.5 kJ mol^{-1}, which is in apparent contradiction to the results obtained by Stickel et al.,[19] who found that rate constants decreased when raising the temperature. The differences on the temperature dependences may be due to the fact that our data show the influence on the abstraction channel while the previous work[19] covers the contribution of both abstraction and addition channels since in that work the temperature dependence was followed in experiments at higher pressures, where the adduct formation is competitive. So we may conclude that the adduct source seems to be inhibited by an increase of temperature driving to thermal decomposition while the abstracting pathway is weakly enhanced, as shown by our results.

Concerning the disagreement between the room-temperature rate constant at 1.0 Torr obtained now, $k(1) = (6.9 \pm 1.3) \times 10^{-11}$ cm^3 molecule^{-1} s^{-1}, and the obtained previously[19], $k(1) = (1.8-3.3) \times 10^{-10}$ cm^3 molecule^{-1} s^{-1} (3−700 Torr), the reason for the discrepancy is unclear. First, pressure conditions in both works are not exactly the same and second, although secondary chemistry could affect the HCl yield when increasing the pressure, numerical simulation[19] indicated that these processes should not be a major source of uncertainty. Our data at low pressure are supported by the results obtained previously for other reactions:

$$CH_3SH + Cl \rightarrow HCl + CH_2SH \qquad (8)$$

$$k(8) = 4.3 \times 10^{-12}\,\text{cm}^3\,\text{molecule}^{-1}\,\text{s}^{-1}\ \text{(ref 38)}$$

$$CH_3SH + Cl \rightarrow HCl + CH_3S \qquad (9)$$

$$k(9) = 1.99 \times 10^{-10}\,\text{cm}^3\,\text{molecule}^{-1}\,\text{s}^{-1}\ \text{(ref 38)}$$

$$CH_3SSCH_3 + Cl \rightarrow HCl + CH_3SSCH_2 \qquad (10)$$

$$k(10) = 6.87 \times 10^{-11}\,\text{cm}^3\,\text{molecule}^{-1}\,\text{s}^{-1}\ \text{(ref 39)}$$

$$CH_3SSCH_3 + Cl \rightarrow CH_3SCl + CH_3S \qquad (11)$$

$$k(11) = 2.02 \times 10^{-10}\,\text{cm}^3\,\text{molecule}^{-1}\,\text{s}^{-1}\ \text{(ref 39)}$$

When the reaction proceeds through addition or abstraction from the hydrogen linked to the sulfur atom, (1b), (9), (11), the rate constants are in the order of 2×10^{-10} cm^3 molecule^{-1} s^{-1}. On the other hand, the rate constants for H-abstraction from the carbon atom are much smaller, (8), (10), with the value of $k(10)$ similar to our result for $k(1a)$.

Comparing the results of the Cl reaction toward DMS with those of OH and NO_3 radicals, with rate constants of $k = 6.1 \times 10^{-12}$ cm^3 molecule^{-1} s^{-1} and $k = 1.0 \times 10^{-12}$ cm^3 molecule^{-1} s^{-1},[34] respectively, the removal of DMS by reaction

1 is very efficient in marine areas, where the Cl concentrations may be in the order of 5×10^3 molecule cm^{-3} or even higher.[15,40] So our results should be taken into account when evaluating the final distribution of products in the DMS degradation. In the atmosphere, the CH_3SCH_2 radicals, (1a), will react almost exclusively with O_2 to give the peroxy-radical

$$CH_3SCH_2 + O_2 \rightarrow CH_3SCH_2OO \qquad (12)$$

$$k(12) = 5.7 \times 10^{-12}\ cm^3\ molecule^{-1}\ s^{-1}\ (ref\ 41)$$

Subsequently the peroxy-radicals are expected to react mainly with NO, NO_2, HO_2, CH_3O_2, or the self-reaction:

$$CH_3SCH_2O_2 + NO \rightarrow CH_3SCH_2O + NO_2 \qquad (13)$$

$$k(13) = 1.18 \times 10^{-11}\ cm^3\ molecule^{-1}\ s^{-1}\ (ref\ 42)$$

$$CH_3SCH_2O_2 + NO_2 \rightarrow CH_3SCH_2O_2NO_2 \qquad (14)$$

$$k(14) = 9 \times 10^{-12}\ cm^3\ molecule^{-1}\ s^{-1}\ (ref\ 41)$$

$$CH_3SCH_2O_2 + CH_3SCH_2O_2 \rightarrow products \qquad (15)$$

$$k(15) = 1.2 \times 10^{-11}\ cm^3\ molecule^{-1}\ s^{-1}\ (ref\ 42)$$

The atmospheric implications of the adduct are extensively analyzed by Urbansky and Wine.[16] Although reactions with NO and NO_2 and the photodecomposition are relatively well-known, there still remain high uncertainties concerning O_2 reactions and thermal decomposition.

Reaction ClO + DMS. Only one study of reaction 2 which reported a room-temperature rate constant of $k(2) = (9.5 \pm 2.0) \times 10^{-15}$ cm^3 $molecule^{-1}$ s^{-1} has been published.[31] In that article the reactions of IO and BrO toward DMS were also investigated with $k = (8.8 \pm 2.1) \times 10^{-15}$ cm^3 $molecule^{-1}$ s^{-1} and $k = (2.7 \pm 0.5) \times 10^{-13}$ cm^3 $molecule^{-1}$ s^{-1}, respectively. Recently, an article by Knight et al,[27] gave $k_{298} = (1.6 \pm 0.3) \times 10^{-14}$ cm^3 $molecule^{-1}$ s^{-1} for the IO reaction. Bedjanian et al.[28] and Nakano et al.[29] have studied the temperature dependence of the BrO−DMS reaction at low pressure. We present here the first temperature-dependence study of reaction 2.

The result for reaction 2 at room temperature obtained in this work, $k(2) = (3.9 \pm 1.2) \times 10^{-15}$ cm^3 $molecule^{-1}$ s^{-1}, is in relative agreement with that reported previously[31] if we take into account the error bars of both studies.

Concerning the products of the reaction, we have only observed quantitative production of DMSO. In separate experiments at 335 K its signal was calibrated by measuring a reference absolute concentration of DMSO coming from a freshly prepared storage balloon of known volume. The flask and all the glass tubing were also heated to prevent losses of DMSO in the walls. The experimental concentrations of DMSO obtained at different times of reaction were higher than the expected [DMSO] calculated with the experimental $k(2)$ assuming that reaction 2 gives DMSO in a unity yield. A similar behavior had been observed in the flow tube study of the BrO−DMS reaction.[28] Then, it was explained assuming that BrO in the wall may react with DMS giving DMSO by an heterogeneous mechanism, which could be written as $BrO + DMS_{wall} \rightarrow DMSO + Br$. This was also envisaged in the study of the DMS−IO reaction.[31] In this work, by simultaneous simulation of the ClO and DMSO profiles, leaving the rate constant of the reaction

$$ClO + DMS_{wall} \rightarrow DMSO + Cl \qquad (16)$$

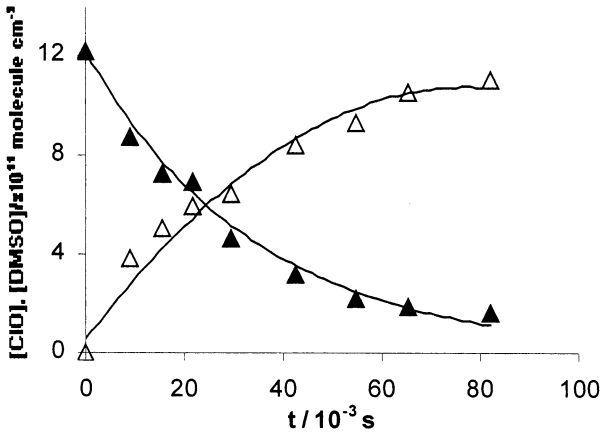

Figure 8. Experimental (points) and fitting (solid lines) data for ClO consumption (▲) and DMSO production (△) in reaction 2 at $p = 1$ Torr, $T = 298$ K, and [DMS] $= 4.39 \times 10^{15}$ molecule cm^{-3}.

as an adjustable parameter, the best fits for different experiments with DMS in the range $(1-5) \times 10^{15}$ molecule cm^{-3} were always obtained for $k_w = 10-12$ s^{-1} (In Figure 8 typical fits of the experimental and simulated profiles are shown). It therefore appears that k_w is constant within the range of [DMS] used; the changes in the rate constants for wall loss and a saturation effect may occur at reactant concentrations lower than those employed here (in fact DMS is used in excess over ClO and so with high concentrations). This is consistent with the linearity k'/[DMS] and the good agreement between k_w obtained by the previous simulation calculations and the experimental intercept found in Figure 6. By subtracting this heterogeneous source of DMSO we have calculated the branching ratio for DMS + ClO → DMSO + Cl as 0.9 ± 0.49.

From these results, chlorine atoms are also quantitatively produced in reaction 2. Indeed, in additional experiments, increasing Cl_2 and ClO concentrations, the formation of CH_3SCH_2Cl (m/e = 96, 98) was observed, which confirms the presence of free Cl atoms and the reaction with DMS, as it was found within the study of reaction 1. These chlorine atoms may undergo reaction with O_3 to regenerate ClO in the reactor, which would have driven to an underestimation of the primary rate constant. However, since the experiments were performed in an excess of DMS over O_3 and the reaction of Cl with DMS ($k_{298} = (6.9 \pm 1.3) \times 10^{-11}$ cm^3 $molecule^{-1}$ s^{-1}) is faster than that with O_3 ($k = 1.2 \times 10^{-11}$ cm^3 $molecule^{-1}$ s^{-1}),[34] Cl atoms will react mainly with DMS. By simulation with FACSIMILE program, the regeneration of ClO was confirmed as negligible.

The relative low value of the preexponential factor and the negative temperature dependence observed for $k(2)$, Figure 7, may be indicative of the formation of an association complex which can then decompose either back to reactants or to give products

$$ClO + CH_3SCH_3 \leftrightarrow [CH_3S(OCl)CH_3]^* \rightarrow CH_3S(O)CH_3 + Cl \qquad (2)$$

Indeed, this behavior has already been observed in the reaction of BrO with DMS.[30] If this is the case, our low-pressure measurement ($P < 2.0$ Torr) may underestimate the real atmospheric rate constant for ClO−DMS since thermalization of the association complex may be inefficient. So the potential importance of reaction 2 could even be larger and kinetic and mechanistic data are also needed at atmospheric pressures.

From a thermodynamic point of view and the calculated $\Delta H_{f,298K}$ for the three reactions XO + DMS → DMSO + X (X

= Cl, Br, I): −95.4, −127.1 and −134.2 kJ mol^{-1} respectively,[34,43] the expected reactivity would be ClO < BrO < IO. This trend is not followed by the IO reaction which may be due to steric effects. The absence of any reactivity trend toward DMS along the ClO, BrO, IO series may also result from the indirect nature of the proposed mechanism. In such a case the measured rate constants depend on many parameters, the rates of the elementary steps involved in the formation and decomposition of the long-lived intermediate.

Since reaction 2 is very slow compared to those of OH, NO_3, and Cl, its direct contribution to DMS removal is negligible. Nevertheless, it could play a potential role through the following chain reaction:

$$ClO + DMS \rightarrow DMSO + Cl \quad (2)$$

$$Cl + O_3 \rightarrow ClO + O_2 \quad (4)$$

$$O_3 + DMS \rightarrow O_2 + DMSO$$

With eq 2 being the limiting step, this process could mean a chlorine-catalyzed destruction of DMS and ozone and an additional source of DMSO, which is formed in the atmosphere mainly from OH−DMS reaction. Ingham et al.[30] evaluated the atmospheric impact of the equivalent sequence with BrO in place of ClO for the marine air of the mid-latitudes and concluded that this catalytic sequence is important. Since the ClO−DMS rate constant is 2 orders of magnitude lower than the BrO−DMS rate constant, the global contribution of ClO to DMS elimination and DMSO formation must be slight. However, BrO−DMS reactions may indirectly increase NO_3 concentrations and so N_2O_5 and $ClNO_2$ which, once photolyzed, would produce a net activation of chlorine chemistry.[30] In this sense our results should also be taken into account in the chemical box models to assess the impact of the reaction between ClO and DMS in the marine boundary layer.

The results reported in this work may help to a better knowledge of the contribution of halogen atoms and halogen oxides to the oxidative capacity of the lower marine troposphere. Nevertheless, the potential role of Cl and ClO in the oxidation of DMS cannot be properly evaluated yet due to the lack of agreement[44,45] in the available data for their concentrations in the marine boundary layer.

Acknowledgment. We thank the European Commission for financial support within the "Energy, Environment and Sustainable Development" V Framework program (EVK2-CT-1999-00033 contract) and the Spanish Ministry of Science and Technology for the PB97-0432 contract.

References and Notes

(1) Barone, S. B.; Turnipseed, A. A.; Ravishankara, A. R. *J. Chem. Soc., Faraday Trans.* **1995**, *100*, 39.
(2) *S-centered radicals*; Alfassi, Z. B., Ed.; Wiley and Sons: Chichester, 1999.
(3) Andreae, M. O. *Marine Chem.* **1990**, *30*, 1.
(4) Spiro, P. A.; Jacob, D. J.; Logan, J. A. *J. Geophys. Res.* **1992**, *97*, 6023.
(5) Ravishankara, A. R.; Rudich, Y.; Talukdar, R.; Barone, S. B. *Philos. Trans. R. Soc. London, Ser. B* **1997**, *332*, 171.
(6) Arsene, C.; Barnes, I.; Becker, K. H. *Phys. Chem. Chem. Phys.* **1999**, *1*, 5463.
(7) Davis, D.; Chen, G.; Bandy, A.; Thornton, D.; Eisele, F.; Mauldin, L.; Tanner, D.; Lenschow, D.; Fuelberg, H.; Huebert, B.; Heath, J.; Clarke, A.; Blake, D. *J. Geophys. Res.* **1999**, *104*, 5765.
(8) Charlson, R. J.; Lovelock, J. E.; Andreae, M. O.; Warren, S. G. *Nature* **1987**, *326*, 655.
(9) Andrea, M. O.; Crutzen, P. *Science* **1997**, *276*, 1052.
(10) Jones, A.; Roberts, D. L.; Woodage, M. J.; Johnson, C. E. *J. Geophys. Res.-Atmos.* **2001**, *106* (D17), 20293.
(11) Venkataraman, C.; Mehra, A.; Mascar, P. *Tellus Ser. B−Chem. Phys. Meteorol.* **2001**, *53* (3), 260
(12) Sørensen, S.; Falbe-Hansen, H.; Mangoni, M.; Hjorth, J.; Jensen, N. R. *J. Atmos. Chem.* **1996**, *24*, 299.
(13) Patroescu, V.; Barnes, I.; Becker, K. H.; Mihalopoulos, N. *Atmos. Environ.* **1999**, *33*, 25.
(14) Butkovskaya, N. I.; Le Bras, G. *J. Phys. Chem.* **1994**, *98*, 2582.
(15) Pszenny, A. P.; Keene, W. C.; Jacob, D. J.; Fan, S.; Maben, J. R.; Zetwo, M. P.; Springer-Young, M.; Galloway, J. N. *Geophys. Res. Lett.* **1993**, *20*, 699.
(16) Urbanski, S. P.; Wine, P. H. *J. Phys. Chem A* **1999**, *103*, 10935.
(17) Falbe-Hansen, H.; Sorensen, S.; Jensen, N. R.: Pedersen, T.; Hjorth, J. *Atmos. Environ.* **2000**, *34*, 1543.
(18) Nielsen, O. J.; Sidebottom, H. W.; Nelson, L.; Rattigan, O.; Treacy, J. J.; O'Farrell, D. J. *Int. J. Chem. Kinet.* **1990**, *22*, 603.
(19) Stickel, R. E.; Nicovich, J. M.; Wang, S.; Zhao, Z.; Wine, P. H. *J. Phys. Chem.* **1992**, *96*, 9875.
(20) Butkovskaya, N. I.; Poulet, G.; Le Bras, G. *J. Phys. Chem.* **1995**, *99*, 4536.
(21) Zhao, Z.; Stickel, R.; Wine, P. H. *Chem. Phys. Lett.* **1996**, *251*, 59.
(22) Kinnison, D. J.; Mengon, W.; Kerr, J. A. *J. Chem. Soc., Faraday Trans.* **1996**, *92* (3), 369.
(23) Resende, S. M.; De Almeida, W. B. *J. Phys. Chem A* **1997**, *101*, 9738.
(24) Wilson, C.; Hirst, D. M. *J. Chem. Soc., Faraday Trans.* **1997**, *93*, 2821.
(25) Langer, S.; McGoveny, B.; Finlayson-Pitts, B.; Moore, R. *Geophys. Res. Lett.* **1996**, *23*, 1661.
(26) Singh, H.; Kasting, J. *J. Atmos. Chem.* **1988**, *7*, 261.
(27) Knight, G. P.; Crowley, J. N. *Phys. Chem. Chem. Phys.* **2001**, *3*, 393.
(28) Bedjanian, Y.; Poulet, G.; Le Bras, G. *Int. J. Chem. Kinet.* **1996**, *28*, 383.
(29) Nakano, Y.; Goto, M.; Hashimoto, S.; Kawasaki, M. *J. Phys. Chem. A* **2001**, *105*, 11045.
(30) Ingham, T.; Bauer, D.; Sander, R.; Crutzen, P. J.; Crowley, J. N. *J. Phys. Chem. A* **1999**, *103*, 7199.
(31) Barnes, I.; Bastian, V.; Becker, K. H.; Overath, R. D. *Int. J. Chem. Kinet.* **1991**, *23*, 579.
(32) Martínez, E.; Aranda, A.; Díaz de Mera, Y.; Rodríguez, D.; López, R.; Albaladejo, J. *Environ. Sci. Technol.* **2002**, *36*, 1226.
(33) Park, J. Y.; Slagle, I. R.; Gutman, D. *J. Phys. Chem.* ***1983***, *87*, 1812.
(34) De More, W. B.; Sander, S. P.; Golden, D. M.; Hampson, R. F.; Kurylo, M. J.; Joward, C. J.; Ravishankara, A. R.; Molina, M. J.; Kolb, C. E. *Chemical Kinetics and Photochemical Data for Use in Stratospheric Modelling*; NASA, JPL California Institute of Technology: Pasadena, CA, 1997.
(35) Kaufman, F. *J. Phys. Chem.* **1984**, *88*, 1409.
(36) Gilliland, E. R. *Ind. Eng. Chem.* **1934**, *26*, 681.
(37) Nicholaisen, S. L.; Friendl, R. R.; Sander, S. P. *J. Phys. Chem.* **1994**, *98*, 115.
(38) Nesbitt, D. J.; Leone, S. R. *J. Chem. Phys.* **1981**, *75*, 4949.
(39) Kambanis, K. G.; Lazarou, Y. G.; Papagiannakopoulos, P. *J. Chem. Soc., Faraday Trans.* **1996**, *92*, 4905.
(40) Wingenter, O.; Kubo, M.; Lake, N.; Smith, T.; Rowland, F. *J. Geophys. Res.* **1996**, *101*, 4331.
(41) Atkinson, R.; Baulch, D. L.; Cox, R. A.; Hampson, R. F., Jr.; Kerr, J. A.; Rossi, M. J.; Troe, J. *J. Phys. Chem. Ref. Data* **1997**, *26*, 1329.
(42) Urbanski, S. P.; Stickel, R. E.; Zhao, Z.; Wine, P. H. *J. Chem. Soc., Faraday Trans.* **1997**, *93*, 2813.
(43) Masuda, N.; Nagano, Y.; Sakiyama, M. *J. Chem. Thermodyn.* **1994**, *26*, 971.
(44) Singh, H. B.; Thakur, A. N.; Chen, Y. E.; Kanakidou, M. *Geophys. Res. Lett.* **1996**, *23* (12), 1529.
(45) Spicer, C. W.; Chapman, E. G.; Finlayson-Pitts, B. J.; Plastridge, R. A.; Hubbe, J. M.; Fast, J. D.; Berkowitz, C. M. *Nature* **1998**, *394*, 353.